ARTICLE NO. 79-0080R

C80-080

Computational Optimization and Wind Tunnel Test of Transonic Wing Designs

00001
20005
20018

H.P Haney* and R.R. Johnson*
Vought Corp., Dallas, Texas

and

R.M. Hicks†
NASA Ames Research Center, Moffett Field, Calif.

A practical procedure for the optimum design of transonic wings is demonstrated. The procedure uses an optimization program based on the method of feasible directions coupled with an aerodynamic analysis program which solves the three-dimensional potential equation for subsonic through transonic flow. Two new wings for the A-7 aircraft were designed by using the optimization procedure to achieve specified surface pressure distributions. The new wings, along with the existing A-7 wing, were tested in the Ames 11 ft transonic wind tunnel. The experimental data show that all of the performance goals were met.

Introduction

THE aerodynamic design of wings for transonic flight has in the past been accomplished by increasing wing sweep and decreasing maximum thickness which often compromises subsonic performance. Dr. Whitcomb at NASA Langley Research Center demonstrated that wing surface contours can be tailored to improve transonic and subsonic performance. These designs were accomplished by experimental methods which are extremely costly and time consuming. Reliable analysis methods for predicting transonic flow fields have recently been developed. R.M. Hicks at NASA Ames Research Center combined transonic flow analyses with an optimization procedure to design efficient airfoils[1] and isolated, three-dimensional wings.[2] The present study extends the three-dimensional optimization procedure to the design of wings with optimum pressure distributions. This paper describes the transonic wing design procedure, its application to two wing designs, and the wind tunnel test of these optimized wings.

A-7 Wing Pressure Prediction

The Jameson potential flow analysis code[3] is used as the aerodynamics analysis for the wing design procedure. It solves the three-dimensional potential equation for subsonic through transonic flow with exact boundary conditions. Therefore, it is capable of treating thick wings with blunt leading edges—the type of wings which were required to meet the performance goals of this study. Before the program was used in the design procedure, it was applied to the prediction of surface pressures on the existing A-7 wing. The objective was to verify that the potential flow, isolated wing aerodynamic program could adequately predict the flowfield about a low aspect ratio wing-fuselage combination and that weak viscous interactions, which exist at all conditions for wind tunnel model testing, would not seriously affect the usefulness of the potential flow solution. Test data obtained in the Vought high speed wind tunnel with a 0.05 scale A-7 model were used for the comparison. The A-7 wing has a leading edge chord extension at 60% of the semispan (Fig. 1). Since the Jameson program requires a continuous leading edge, the discontinuity was replaced by a smooth curve. The predicted pressures show excellent agreement with test data. A representative comparison of the chordwise pressure distributions at 75% of the semispan is presented in Fig. 2. The forward 28% of the chord is drooped 7 deg nose down. The pressures on the upper surface are particularly sensitive to the resulting discontinuity, but the analytical results show a very good prediction of the velocities in that region. A comparison of the predicted and experimental pressures at 20% of the semispan is presented in Fig. 3. Even at that location, where fuselage effects often produce noticeable deviations from an isolated wing analysis, the comparison is good.

Airfoil Optimization

Prior to the finite wing optimization study, transonic airfoils were optimized and evaluated for use as wing sections in the starting three-dimensional wing geometry. That procedure and the results are summarized here in order to demonstrate an application of numerical optimization to a simpler two-dimensional problem and to describe the geometric functions and design variables which were subsequently used for the three-dimensional wing optimization. In addition, the procedure shows the results of using a passive displacement thickness approximation to the boundary layer, an approximation which was also used in the finite wing design study.

A schematic flow chart of the numerical optimization design program is shown in Fig. 4. An iterative solution of the full potential equation for two-dimensional transonic flow[4] was used for the aerodynamic analysis program. A baseline airfoil is required to start each design problem. The airfoil shape is represented in the program by the following equation:

$$Y = Y_{\text{basic}} + \sum_i a_i F_i$$

where Y_{basic} is the set of ordinates of the baseline airfoil and F_i are the shape functions (Fig. 5). The shape functions are

Presented as Paper 79-0080 at the 17th Aerospace Sciences Meeting, New Orleans, La., Jan. 15-17, 1979; submitted Feb. 26, 1979; revision received July 6, 1979.

Index categories: Aerodynamics; Computational Methods; Transonic Flow.

*Engineering Specialist, Flight Technologies. Member AIAA.

†Research Scientist, Aerodynamics Research Branch. Member AIAA.

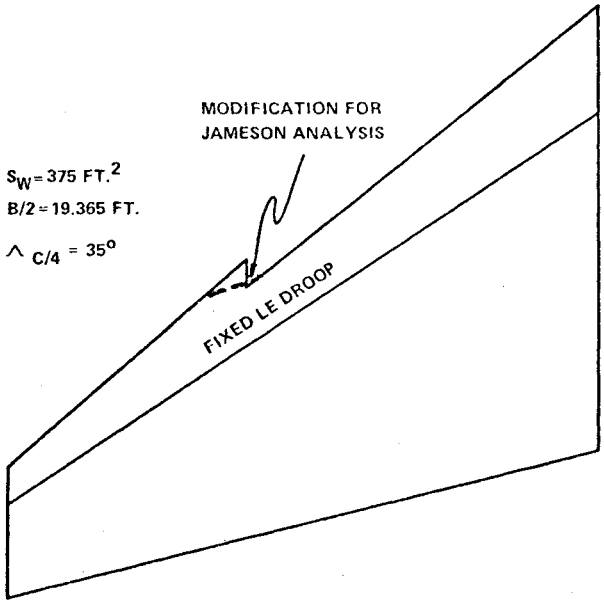

Fig. 1 A-7 wing planform.

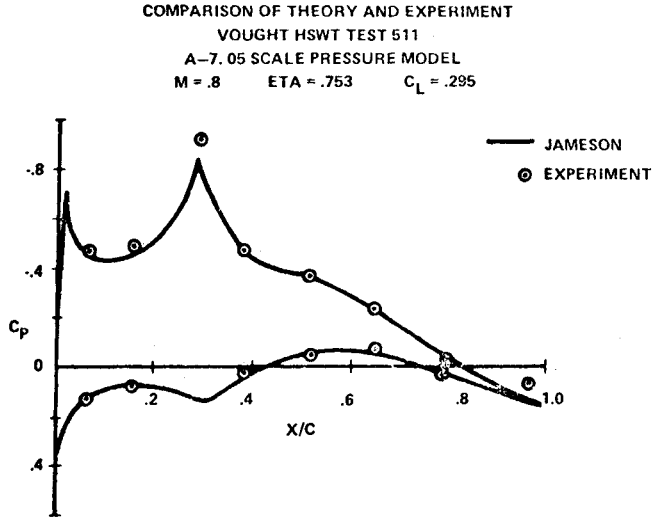

Fig. 2 A-7 wing chordwise pressure distributions.

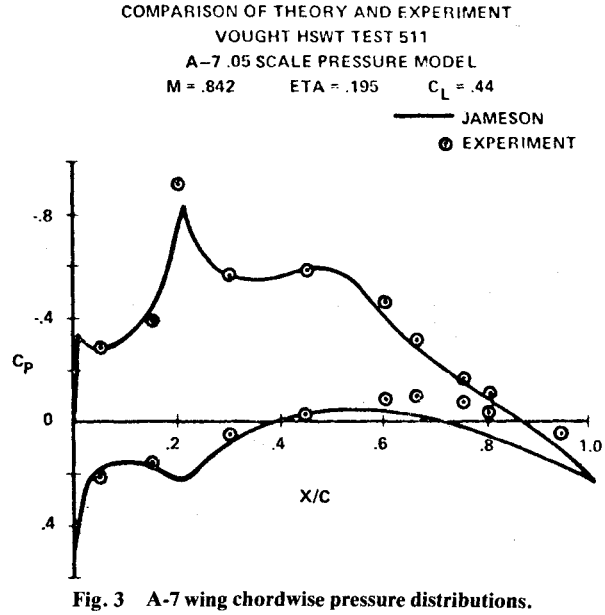

Fig. 3 A-7 wing chordwise pressure distributions.

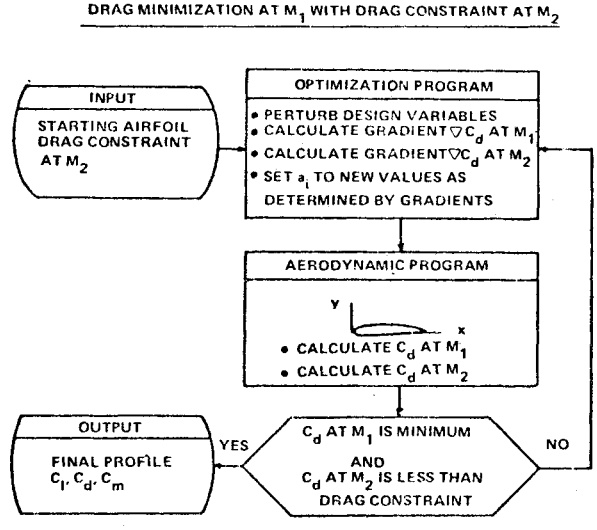

Fig. 4 Flow chart of numerical optimization design program.

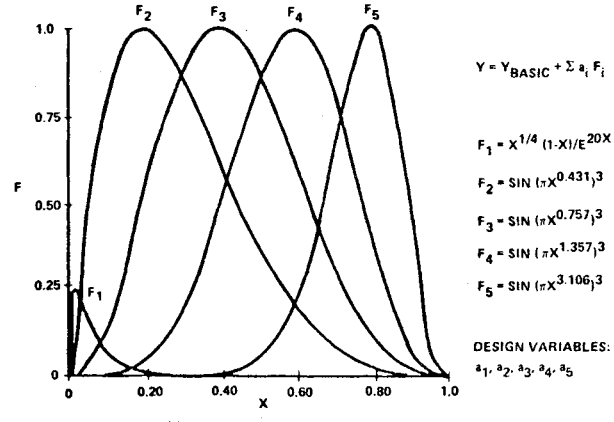

Fig. 5 Airfoil shape functions.

added linearly to the baseline profile by the optimization program[5] to achieve the desired design improvement. The contribution of each function is determined by the value of the coefficient a_i associated with that function.[6] The a_i coefficients are therefore the design variables. Other inputs to the program include Mach number, angle of attack, and any constraints to be imposed on the design.

The hypothetical design problem represented by the flow chart is drag minimization at one Mach number, M_1, with drag constrained to some specified value at another Mach number, M_2. The optimization program changes the design variables, one by one, and returns to the aerodynamics program for evaluation of the drag coefficient at both Mach numbers M_1 and M_2 after each change. The partial derivatives of drag with respect to each design variable form the gradient of drag, ∇C_d. The initial direction in which the design variables are changed to reduce the drag coefficient at M_1 is $-\nabla C_d$ (the steepest descent direction) if the drag constraint at M_2 is not active. The optimization program then increments the design variables in this direction until the drag starts to increase or the drag constraint at M_2 is encountered. If either of these possibilities occurs, new gradients are calculated and a new direction is found which will decrease drag without violating the constraint. When a minimum value of drag for M_1 is attained with a satisfied drag constraint at M_2, the required optimized airfoil has been achieved.

The value of considering off-design performance of an airfoil during the design process will be illustrated by comparing the results of a single design point optimization with a double design point optimization. The first involves recon-

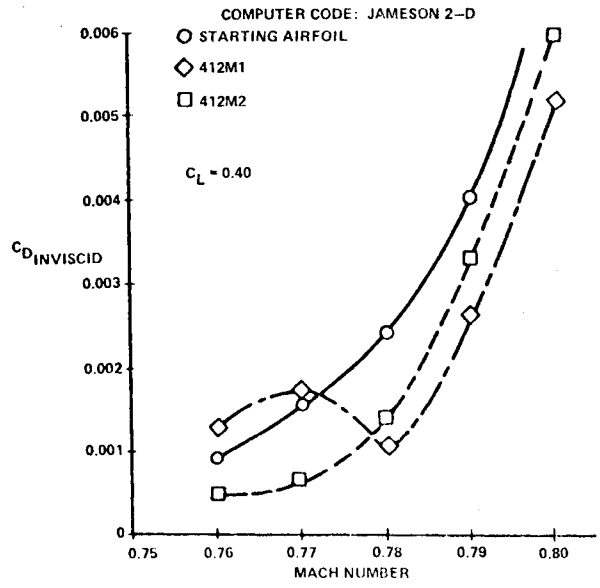

Fig. 6 Airfoil section optimization.

touring the upper surface of an existing supercritical airfoil to reduce the wave drag at a single design Mach number. The second consists of recontouring the upper surface of the same airfoil to reduce the wave drag at the design Mach number subject to a drag constraint at a lower Mach number.

The calculated wave drag for Mach numbers near drag divergence for the starting airfoil and the two optimized airfoils is presented in Fig. 6. All these data are for 0.40 C_l, the design lift coefficient of the starting airfoil. Mach number 0.78 was arbitrarily selected as the primary design point, i.e., the Mach number at which the drag would be minimized. Results of the single design point optimization are indicated at 412M1. The drag at Mach number 0.78 is significantly less than that of the starting airfoil and, as a result, the drag rise occurs at a higher Mach number. However, the drag at lower Mach numbers, 0.76 and 0.77, is greater than that of the starting airfoil. This local region of drag creep could limit the usefulness of the improved drag rise Mach number of the optimized airfoil.

In order to avoid the drag-creep problem, the airfoil was optimized a second time with an upper bound of 0.0005 imposed on the drag coefficient at Mach number 0.77. Results of this double design point optimization are indicated in Fig. 6 as 412M2. The drag rise for this airfoil occurs at a slightly lower Mach number than it does for 412M1, but there is no drag-creep over the range of Mach numbers for which the airfoils were analyzed. Therefore, airfoil 412M2 is the more desirable design. The geometric modification is shown in Fig. 7. The change is primarily a reduction in surface curvature from 5 to 40% of the chord.

The aerodynamics code that was used in the optimization program is an inviscid, potential flow analysis method. In order to account for first-order viscous effects in the flowfield solution, a boundary layer displacement thickness was added to the starting profile before the optimization process. The displacement thickness was calculated for the pressure distribution of the starting airfoil at a Mach number near its design condition, 0.78. It remained unchanged throughout the optimization process, and each of the optimized airfoils included this same passive displacement thickness. Therefore, the analytical characteristics of the airfoils did not reflect potential changes in boundary layer behavior due to changes in the chordwise pressure distributions.

Models of the starting airfoil and airfoil 412M2 were tested in the NASA Ames 2×2 ft wind tunnel. The experimental data from that test agree very well with the analytical predictions.

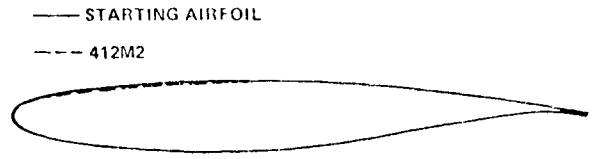

Fig. 7 Airfoil geometry comparison.

Wing Design Goals

Two new wings were designed for the A-7 which demonstrate how transonic computational design methods can improve overall aircraft performance. The design goal for the first wing was to increase the A-7 wing thickness by 71% while maintaining the same drag divergence Mach number. The design goal for the second wing was to reduce the induced drag by 25% and to increase the wing thickness by 28% while maintaining the same drag divergence Mach number. Preliminary analytical studies with the Jameson three-dimensional program indicated that if section properties could be optimized successfully, design goals for the first wing, wing 1, could be achieved with the same planform as the existing A-7 wing: aspect ratio 4, 35 deg quarter chord sweep. The starting streamwise sections were defined by a 12% thick, supercritical airfoil which, when adjusted for planform effects with simple sweep theory, had a design lift coefficient consistent with the performance objectives of the first wing. That 12% thick airfoil was the same as the starting airfoil which was evaluated during the airfoil optimization study.

An aspect ratio of 5 was selected for wing 2, based upon aircraft performance studies. The Jameson program indicated that an optimized wing which was 28% thicker than the A-7 wing could have as little as 20 deg of quarter chord sweep without changing the drag divergence Mach number. The starting streamwise sections were defined by a 9% thick, supercritical airfoil which had a design lift coefficient consistent with the performance objectives of the second wing.

Wing Optimization Procedure

The Jameson three-dimensional analysis program was used to evaluate the initial geometries of both new wings, which consisted of a 12% thick, supercritical airfoil in the wing 1 planform and a 9% thick, supercritical airfoil in the wing 2 planform. As expected, the chordwise pressure distributions for both wings were significantly different than the highly efficient two-dimensional pressure distributions of the respective airfoils. The greatest differences existed near the centerline and near the wing tip, caused by the finite span induced flowfield. Wing sweep and taper also degraded the flowfield across the entire span of each wing.

In order to synthesize a wing design procedure, the Jameson three-dimensional code FL022, was used for the aerodynamic analysis program within the optimization code. It is based on an iterative solution of the full potential equation for three-dimensional transonic flow. Viscous effects are not modeled in the program. A two-dimensional boundary layer displacement thickness was added to the sections which were used to define the starting wing geometry. It was calculated for a representative pressure distribution of the starting wing and remained unchanged throughout the optimization process. The displacement thickness was subtracted from the final wing geometry.

Twist, trailing edge camber, and 22 surface shape functions at each of five semispan stations were used as the design variables. The trailing edge camber variable was represented as a nonlinear meanline displacement function for control of the aft loading. It was of the form $\Delta y/c\alpha\,(x/c)^{8}$. The surface shape functions were of the same form as those used for the two-dimensional airfoil optimization and were applied to the upper surface and lower surface at each defining station. The exponents (on x/c) in the sine function expressions were

assigned so that the maximum perturbations were at 5, 10, 20, 30, 40, 50, 60, 70, 80, and 90% of the chord. Two exponential decay functions provided variations in curvature near the leading edge. These particular shape functions were selected because of previous success in optimizing two-dimensional sections with functions of the same type.

During a preliminary series of wing optimization runs, drag coefficient was selected as the parameter to be minimized. The runs were effective in reducing drag, but adverse pressure gradients which existed in the velocity distributions on the starting wing still remained after the optimization runs. The gradients were quite large and would have caused premature boundary layer separation. To achieve wing geometries with pressure gradients weak enough to avoid separation, desired pressure distributions were specified over the entire chord and substituted for drag coefficient as the design goal. Specifically, the square of the difference between the existing pressure distribution and a desired pressure distribution was integrated over the entire chord and specified as the parameter to be minimized (Fig. 8).

The shapes of the desired pressure distributions were patterned after two-dimensional, supercritical airfoil distributions which are known to avoid premature boundary layer separation over a wide range of flight conditions. The pressure levels at each defining section were tailored to the thickness-to-chord ratio and design lift coefficient of each wing. An upper surface maximum local Mach number of 1.17 was specified to be the same at all defining stations except for the centerline station, where the maximum Mach number was reduced a small increment to reduce the expected adverse wing-body interference effects. Thus, straight isobars over most of the upper surface were a design objective. The lower surface levels were varied at each defining station to force the spanwise loading distribution to be elliptical and, thereby, to achieve minimum induced drag. Overall, the optimization objective for these transonic wings was to restore the efficient, supercritical airfoil pressure distributions which had been changed by the three-dimensional effects.

Since optimization of the entire wing in one computer run would have been impractical, wing sections at each of the defining stations were optimized sequentially from root to tip, first on the upper surface and then on the lower surface. For the first wing, a single pass across the wing produced chordwise and spanwise loading distributions which were sufficiently close to the desired loadings to achieve the aerodynamic performance goals. The relatively high sweep of the wing, 35 deg at the quarter chord, prevented velocity distribution changes at the outboard sections from disturbing the previously optimized inboard section velocity distributions. For the second wing, which has only 20 deg sweep at the quarter chord, optimizations at the outboard sections did affect the previously optimized inboard sections. As a result, a second optimization pass across that wing was necessary. For both wings, it was found that when all the design variables at a given section were active, the optimization progressed slowly. Computer runs with only twist and trailing edge camber as the active variables produced good results. In addition, selection of a limited number of surface shape functions based upon a comparison of desired vs starting pressures effectively expedited the optimization and reduced costs. Optimization of each wing section required approximately 2 h of CDC 7600 computer time. Therefore, the complete wing designs required about 10 h each.

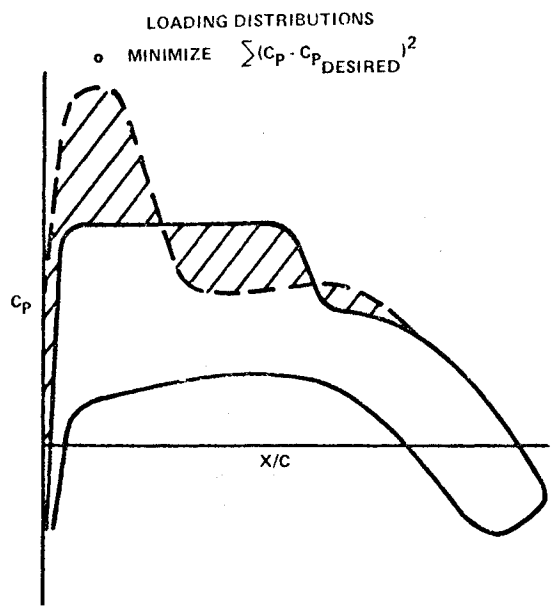

Fig. 8 Use of optimization code for wing design.

Wing Design Results

The starting and final wing geometry and pressures for wing 2 are presented in Figs. 9–11. At the wing centerline (Fig. 9), the optimization code has produced a section with its maximum thickness at 20% of the chord. (The maximum thickness of the starting section is at 38%.) The aft camber has been removed and the section has been twisted significantly. The resulting chordwise pressure distribution

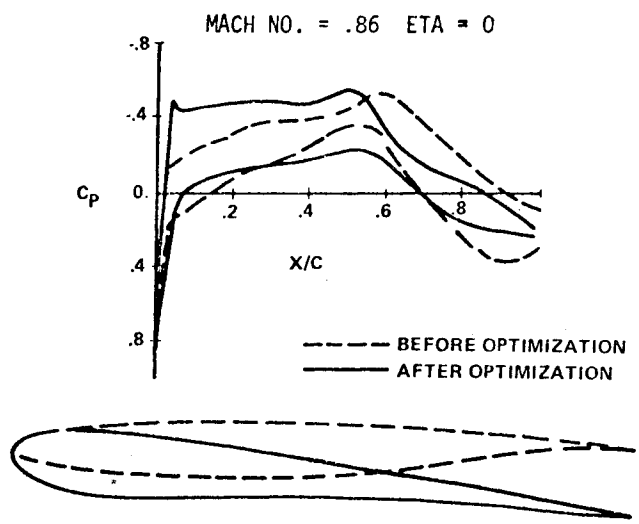

Fig. 9 Wing 2 starting and optimized geometry and pressures.

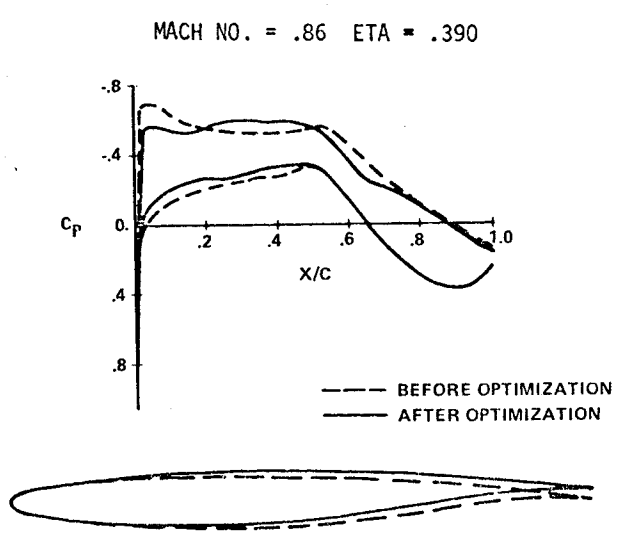

Fig. 10 Wing 2 starting and optimized geometry and pressures.

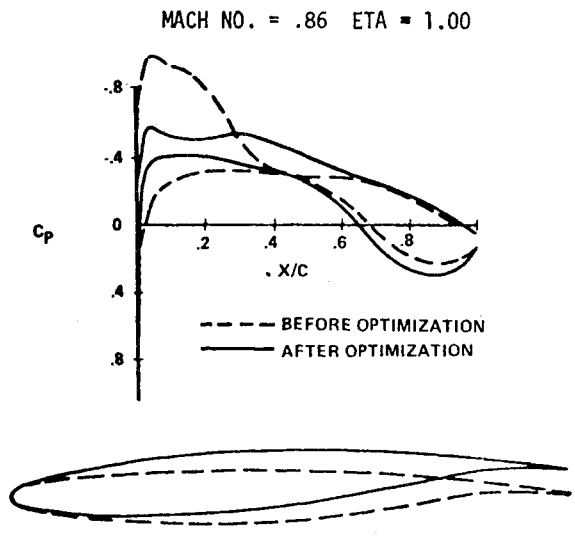

Fig. 11 Wing 2 starting and optimized geometry and pressures.

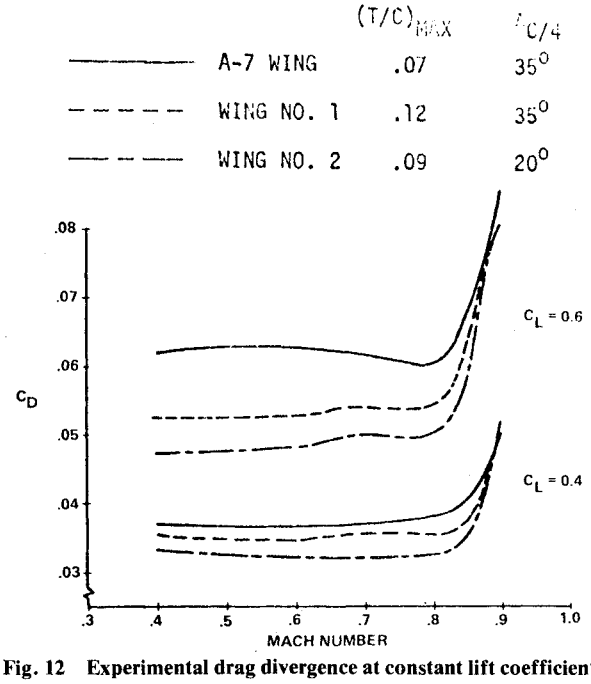

Fig. 12 Experimental drag divergence at constant lift coefficients.

has most of the desirable features of an efficient supercritical airfoil: 1) supersonic flow begins near the leading edge on the upper surface, providing a significant lift contribution from the forward portion of the wing; 2) moderate supersonic flow is maintained to approximately the midchord, where it is decelerated through a weak shock; and 3) lift is generated by aft camber, but without excessively adverse pressure gradients.

It is interesting to note that the analytically optimized geometry is similar to root section designs produced by extensive transonic wind tunnel testing. As expected, less optimization was required at midspan stations where the flow is more nearly two-dimensional (Fig. 10). Although the pressure distribution at the tip was significantly improved through contouring and washout, further improvement is needed (Fig. 11). The optimization changes to wing 1 were similar to those for wing 2.

Wind Tunnel Test

Models of the two optimized wings were tested in the NASA Ames 11 ft transonic wind tunnel during July 1978. The existing A-7 wing was also tested to provide baseline data for comparison. The primary purpose of the test was to determine the transonic longitudinal characteristics of the baseline wing and the two optimized wings.

The David W. Taylor Naval Ship Research and Development Center (DTNSRDC) 0.1 scale A-7 flow-through model was modified to accept pressure models of the two optimized wing designs. Three 48 port scanivalves were placed in the fuselage nose, and a wing root bending moment gage was added to the existing A-7 force wing model. Both optimized wing models have 120 static pressure taps distributed along four spanwise stations of the left wing and wing root bending moment strain gages. No leading or trailing edge devices were built into the two pressure wings.

The optimized wing model contours were machined to closely simulate the mathematical representation used in FL022. Linear surface elements connect the optimized airfoil sections along lines of constant x/c. The theoretical wing center section is actually submerged within the fuselage. This deviation of the wind tunnel model from the optimized isolated wing was not noticeable on wing 2, which had a significant twist change near the centerline.

Pitch polars were run with each of the three wing models on the A-7 fuselage at Mach numbers of 0.4, 0.6, 0.7, 0.8, 0.85, 0.88, and 0.9 for 6×10^6 Reynolds number and Mach numbers of 0.7, 0.8, 0.85, 0.88, and 0.9 for 8×10^6 Reynolds number. Additional data points were taken near 0.4 and 0.6

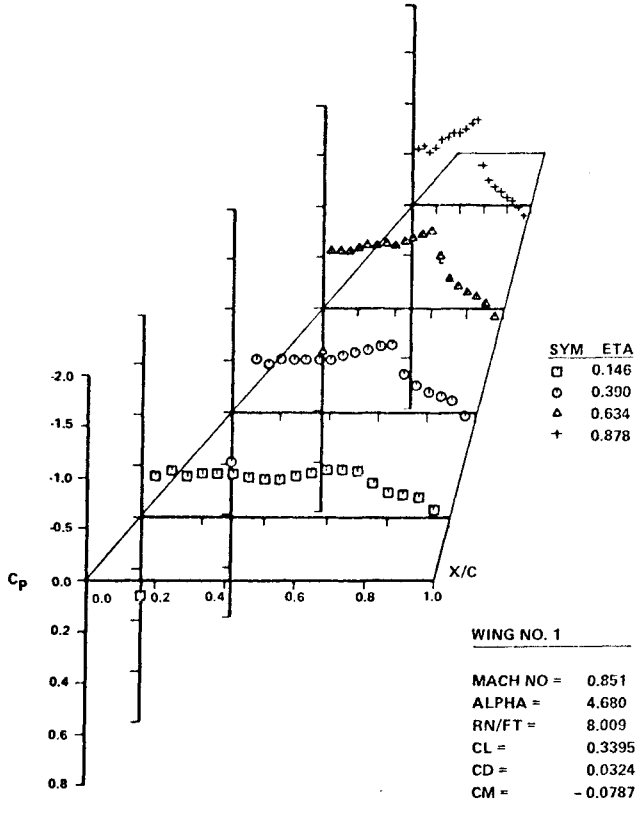

Fig. 13 NASA Ames test 231-1-11 upper surface pressure distribution.

C_L at Mach numbers of 0.75, 0.82, 0.84, 0.86, 0.87, and 0.89 for 8×10^6 Reynolds number to define drag divergence Mach numbers accurately. Oil flow studies were made of the two optimized wings. Photographs of the upper and lower surfaces of the left wing were taken at Mach numbers of 0.6, 0.8, 0.85, and 0.88 at angles of attack.

Six component balance data and wing root bending moment buffet data were taken for each wing at all data points. Pitching moment was referenced to 30% of the A-7 mean geometric chord. Pressure data were also taken for the

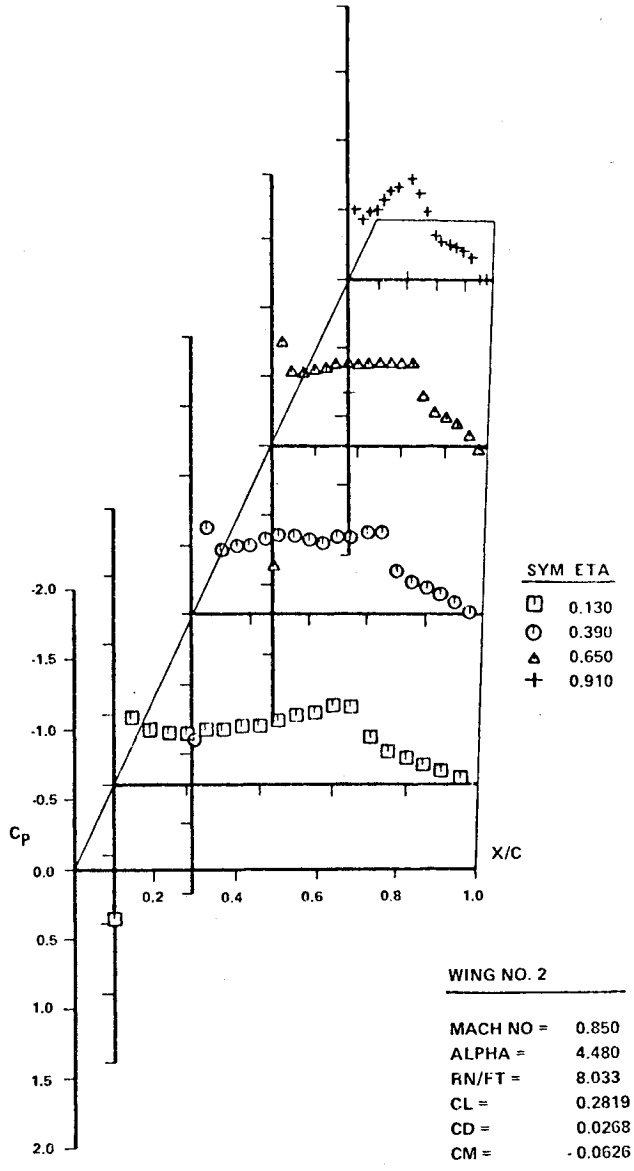

Fig. 14 NASA Ames test 231-1-11 upper surface pressure distribution.

two optimized wings except during oil flow studies. Grounding between the balance sting and model at high C_L and dynamic pressures limited the test angle of attack.

Test Results

Drag coefficients as a function of Mach number for the three wing configurations are presented in Fig. 12. These data for constant lift coefficients of 0.4 and 0.6 show that the drag divergence Mach numbers of wings 1 and 2 are the same as the drag divergence Mach number of the A-7 wing configuration and, therefore, that the primary design goals have been achieved. For Mach numbers below drag divergence, these curves show that the drag of the new wings is significantly less than the drag of the A-7 wing.

Upper surface pressure distributions for wing 1 at Mach 0.85 are presented in Fig. 13. These data show that the shock strength remains weak and the boundary layer remains attached, even though the lift is being generated by large regions of locally supersonic flow on the upper surface. It is this desirable feature that distinguishes this optimized transonic wing from conventional high speed wings. Upper surface pressure distributions for wing 2 at Mach 0.85 are presented in Fig. 14. These data show the same desirable supercritical features as were observed in the pressure distributions of wing 1.

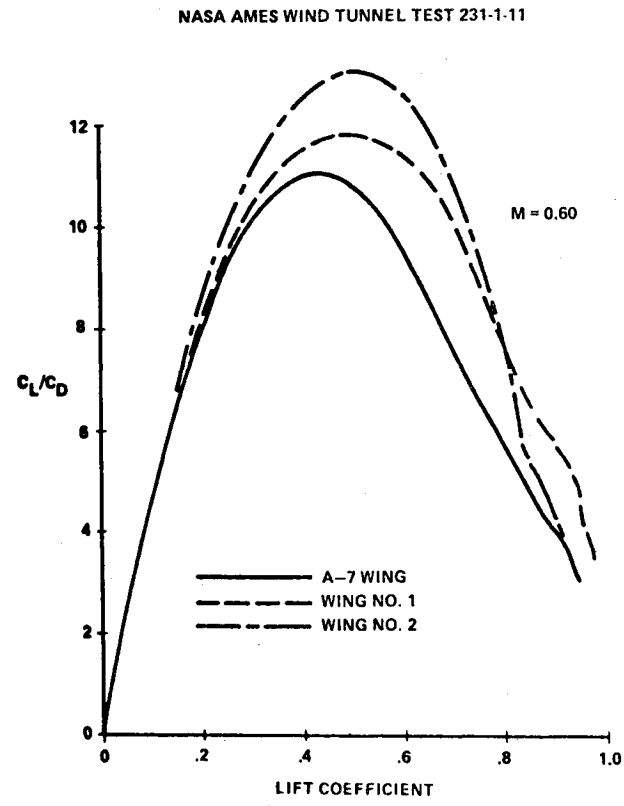

Fig. 15 Experimental lift/drag ratio at Mach number 0.60.

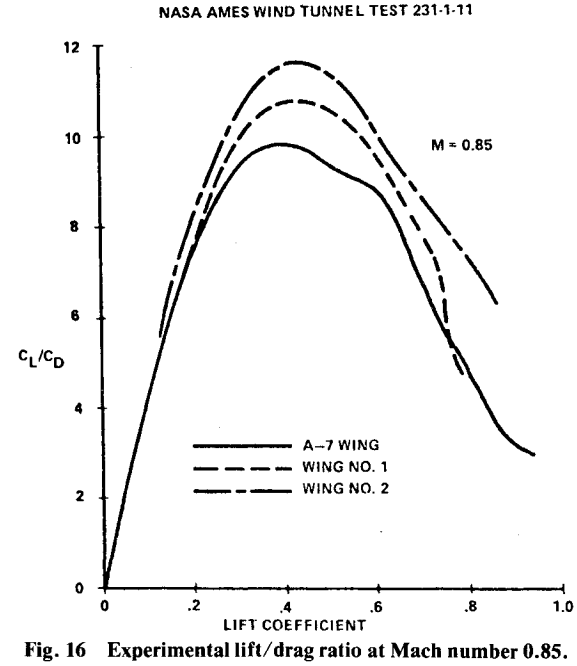

Fig. 16 Experimental lift/drag ratio at Mach number 0.85.

Lift-to-drag ratios for the three wing configurations are presented in Figs. 15 and 16. At Mach number 0.6, both of the optimized wings have substantially higher L/D than the A-7 wing, except for wing 2 at lift coefficients above 0.9. At Mach 0.85, values of L/D for the optimized wings are greater than those for the A-7 wing, but the amount of improvement is somewhat less than at the lower Mach number. At Mach numbers above drag divergence, 0.88 and 0.90, the data showed that the aerodynamic efficiency of the new wings is less than that of the A-7 for much of the C_L range. That characteristic is typical of thicker wings, since they are more sensitive to shock-induced separation at Mach numbers above drag rise.

Conclusions

A numerical optimization procedure for transonic wing design has been demonstrated. Two new wings for the A-7 aircraft were designed by using the optimization procedure to achieve specified surface pressure distributions. Wind tunnel test data showed that all of the design goals were met or exceeded. The following conclusions are emphasized.

1) An aerodynamic design procedure consisting of Jameson's three-dimensional, transonic flow analysis code and a numerical optimization algorithm is a powerful tool for transonic wing design.

2) The technique of designing to specified pressure distributions is an effective way to control the shock wave strength and location, and to avoid premature boundary layer separation. This method is particularly important when the aerodynamic analysis code does not simulate viscous effects.

Acknowledgments

Portions of this study were performed under NASA Contract NAS2-9653 and DTNSRDC funding. The assistance of Ray Siewert, Gary Chapman, Paul Scheurich, Joe Martin, and Jonah Ottensoser is gratefully acknowledged.

References

[1] Hicks, R.M., Murman, E.M., and Vanderplaats, G.N., "An Assessment of Airfoil Design by Numerical Optimization," NASA TMX-3092, 1974.

[2] Hicks, R.M., and Henne, P.A., "Wing Design by Numerical Optimization," AIAA Paper 77-1247, Aircraft Systems and Technology Meeting, Seattle, Washington, August 22-24, 1977.

[3] Jameson, A., Caughey, D.A., Newman, P.A., and Davis, R.M., "A Brief Description of the Jameson-Caughey NYU Transonic Swept-Wing Computer Program—FL022," NASA TMX-73, 996, Dec. 1976.

[4] Jameson, A., "Iterative Solution of Transonic Flows over Airfoils and Wings Including Flows at Mach 1," *Communications on Pure and Applied Mathematics,* Vol. 27, 1974, pp. 283-309.

[5] Vanderplaats, G.N., "CONMIN-A Fortran Program for Constrained Function Minimization, User's Manual," NASA TMX-62, 282, Aug. 1973.

[6] Hicks, R.M. and Vanderplaats, G.N., "Application of Numerical Optimization to the Design of Supercritical Airfoils without Drag-Creep," SAE Paper 770440, 1977.